PAPER 64 (SESSION V)

Corrosion-fatigue crack propagation

REGIS M. N. PELLOUX

Boeing Scientific Research Laboratories
Seattle, Washington State, U.S.A.

Summary

The influence of environment on the mechanisms of fatigue crack propagation in aluminum alloys was studied in vacuum, ambiant air, distilled water and sea water. A model is presented which shows that in the absence of corrosion, fatigue crack propagation is the result of crack extension by alternating shear. A correlation between crack tip opening displacements and crack growth rates is established. The model also accounts for the fact that fatigue striations are not created when the tests are performed in vacuum. The crystallographic nature of fatigue cracking is shown by means of etch pits.

The influence of the corrosive environment on fatigue crack propagation is determined by measuring the change of striation spacings as an impressed corrosion current is reversed. The formation of ductile or brittle striations can be controlled by making the specimen successively cathodic and anodic. The overall plan of fracture changes its orientation at each current reversal. The susceptibility to corrosion during fatigue of the aluminum alloys is shown to be strongly dependent on the ageing treatment. For all the alloys the instantaneous change of the type of fracture (shear to cleavage) when the current is reversed (cathodic to anodic) shows that during fatigue crack propagation corrosion influences the mode of fracture by an adsorption process.

Introduction

It is customary to divide the process of fatigue crack propagation into two stages. Stage I corresponds to the propagation of a crack along crystallographic planes approximately parallel to the plane of maximum shear stress. Subsequently, during Stage II the plane of crack propagation is at 90 degrees to the axis of maximum tensile stress. This work reports on the influence of environment on the mechanisms of crack propagation during Stage II. The Stage II fatigue fracture surface is usually covered with fatigue striations running parallel to the front of crack propagation. Following a designation established by Forsyth (1) fatigue striations are usually classified in two categories: ductile striations and brittle striations. Fig. 1 is a typical illustration of the two types of striations juxtaposed in two neighboring grains in an A1-Zn-Mg alloy tested in distilled water at room temperature. Ductile striations have been the subject of extensive work and review by Forsyth [1], Laird [2], Hertzberg [3] and Meyn [4]. Brittle striations have been studied mainly by Forsyth [1]. who showed they form predominantly in the presence of a corrosive environment. The present work is a study of the influence of vacuum, air, distilled water and sea water on the mechanisms of formation of ductile and brittle striations in aluminum alloys.

Fatigue crack propagation is the repetitive process of extension of a sharp crack since crack tip resharpening takes place at each cycle during unloading. Consequently we shall first review briefly the mechanisms of deformation taking place at the tip of a sharp crack. For simplicity that by sharp crack is defined as a crack with a tip radius smaller than the width of a slip or shear band.

Deformation at the tip of a sharp crack

During fatigue crack propagation, plastic deformation is limited to a small region near the crack tip and the remainder of the structure is elastic. Close to the tip of the crack the plastic strains are very large compared to the elastic strain. This means that fully plastic specimens with sharp cracks may be used to simulate and understand the processes of deformation at the tip of the crack. The fact that the rate of crack growth per cycle, that is the spacing of a striation is about 1/200th to 1/1000th of the plastic zone size also makes this assumption realistic. To make our model easier to analyze, we shall assume that the material is a rigid-plastic solid.

The simplest fully plastic specimen is a single edge notch plane strain tensile bar as shown on Fig. 2a. The plasticity solution of the mechanics of deformation has been given by McClintock [5] and shows that deformation can take place only by shear on the two planes AB and AC. Deformation can proceed either alternately on one band and then on the other or simultaneously since the exact solution does not specify as to how the shear is distributed between the two planes. Figs. 2b and 2c show that if shear starts on plane AB and if there is some strain hardening on that plane, it will be easier for the shear to proceed on a second plane AB′ which has not been deformed so that the shear would tend to be alternating. This process of deformation by alternating shear results in an extension of the notch length by a mechanism of rupture and not by fracture. The absolute extension of the crack length is equal to half the displacement of the flanks of the notch, i.e. half the crack tip opening displacement. This sliding leads to the formation of a 90° notch tip which remains always sharp regardless of the magnitude of the alternating shear displacement. The displacement could be as small as a Burgers vector in a crystal or as large as a macroscopic shear in a continuum. The newly created 90° flanks of the notch do not show the successive shear displacements as slip steps or other markers. In the case of deformation by alternating shear the deformation process should be entirely reversible at least in theory. However, in practice the fact that the freshly exposed crack surface for most metals is immediately oxidized in air will limit the amount of reversibility of the deformation at the tip.

The double edge, sharply notched, fully plastic tensile specimen gives a better representation of the real elastic-plastic crack tip behavior than the single edge notched tensile specimen. Fig. 3 shows the flow field of the double edge notched specimen. In the first stage of deformation of this

tensile specimen, i.e. before the slip line flow field is markedly changed, the crack length is extended by shear by an amount U for a crack tip opening displacement $2U$. Further sliding then leads to blunting of the tip which creates a large strain concentration ahead of the crack tip resulting in fracture.

The solution obtained for crack extension by alternating shear for the two types of specimens mentioned above, works reasonably well in reality even for materials with some strain hardening. Experiments were performed with fully plastic tensile specimen of pure aluminum and pure copper [5] and a region of sliding off was always observed at the root of the sharp notch. This region is characterized by the absence of fracture by voids although second phase particles are present and the presence of slip lines parallel to the crack front. These markings were called serpentine slide by Beachem [6]. The region of sliding off is always followed by a region of dimples where fracture takes place by void coalescence as the result of the strain concentration due to blunting of the tip [5].

So far we have supposed that for a finite crack tip opening displacement crack extension of a sharp crack can take place only by shear, i.e. by a process of rupture. However, crack extension could also take place by tensile fracture, i.e. by cleavage for a crystalline material. If crack extension takes place by cleavage during fatigue it must be accompanied by a certain amount of shear or sliding in order to arrest the crack at each cycle.

As shown in the following section, the relative amount of crack extension by shear and cleavage depends markedly on the slip character of the material and also on the environment.

Fatigue crack growth rates and crack tip opening displacements

Fig. 2 shows that for a crack tip opening displacement $2U$ the crack extension relative to the whole width of the fully plastic bar is $2U$. A relationship between crack tip opening displacement and fatigue crack growth rate has been the basis of many dislocation models used for the theoretical calculation of a fatigue crack growth law. McClintock [7] compared calculated values of crack tip opening displacements and measured striation spacings and found that the growth rate was equal to half the crack tip opening displacement. In order to compare crack tip opening displacement (CTOD) to fatigue crack growth rates on the basis of the model of Fig. 2, we have to assume that the striation spacing is approximately equal to the macroscopic growth rate. This was not the case for the data used by McClintock; however, our recent work shows that, in general, the striation spacing and the macroscopic rates at a given crack length are roughly equal. The crack tip opening displacement $2Vy$ can be calculated by using Williams equations [8]

$$2Vy = \text{plastic zone size} \times \text{yield strain}$$

In the case of fatigue, i.e. with reversed flow, the yield strength should be taken as $2Y$ (see Rice [9]), consequently the reversed plastic zone size in fatigue is given by

$$R = \frac{(\Delta K)^2}{2\pi(2Y)^2}$$

and the crack tip opening displacement by

$$2Vy = R \times \frac{2Y}{E}$$

$$2Vy = \frac{(\Delta K)^2}{2\pi(2Y)E}$$

Y is the yield strength, E the modulus of elasticity.

Fig. 4 shows the broad bands of data representing the relationship between typical fatigue crack growth rates in air and amplitude of the stress intensity factor for some aluminum alloys [10], titanium alloys [10] and a 4340 steel [11]. The calculated crack tip opening displacements corresponding to the data of Fig. 4 are plotted against crack growth rates on Fig. 5. It appears that there is a unique relationship between CTOD and fatigue crack growth rates as suggested by Fig. 2. The relationship between crack tip opening displacements and growth rates is not linear as predicted by the model of Fig. 2 but it can be written

$$\text{Growth rate} = \text{constant} \times (\text{crack length})^2$$
$$\text{Growth rate} = \text{constant} \times (\text{CTOD})^2$$

The discrepancy cannot be explained at this time, but the value of $2Vy$ calculated by Williams [8] equation is a very rough approximation of the CTOD. It is good only for relative comparisons. The residual stresses around the tip and along the fracture surfaces may account for the l^2 and $(\text{CTOD})^2$ dependance. It is interesting to note that the calculated CTOD is smaller than the growth rate below 5×10^{-5} inches and larger than dc/dn above 5×10^{-5} inches.

Further evidence that fatigue crack propagation rates are related to crack tip opening displacements is demonstrated by the results of programmed load tests reported previously [12]. There is a one to one correlation between the widths of the ductile striations and the load and maximum load levels. A change of load amplitude or maximum load level results in an immediate (no delay) change of striation width as would be expected if the amount of crack extension is directly related to the amount of CTOD. For a given CTOD the amount of crack extension will certainly depend on the mechanical properties of the material at the crack tip (ductility, work hardening) and on the environment.

Ductile striations

Crystallographic nature of ductile striations in aluminum alloys

In FCC metals slip takes place on {111} type planes in a 110⟩ type direction. By comparing Fig. 2 and the slip systems in a FCC alloy it can be seen that the crystallographic orientation which can best satisfy the continum flow fields is that given in Fig. 6a. This means that in the case of repeated shear rupture the crack tip should be parallel to a ⟨110⟩ direction and the plane of crack propagation should be a [100] type plane. Fig. 6b shows the relative orientations of the slip planes, the crack front and crack plane if the proposed model is operating. Hertzberg [3] had suggested a similar model which lacked experimental evidence.

Etch pitting of the fracture surfaces of aluminum was used to determine the change of orientation of the crack front from grain to grain. The etching reagent is 50 water, 50 HNO_3, 32 HCl, 2HF. With 2024T3 etch pits were easily obtained, the etching reagent attaching preferentially the [111] planes. Fig. 7 shows the pyramidal etch pits obtained, the side faces being [111] plane and the base a [100] plane. The edges of the basal plane are ⟨110 type ⟩ direction. It can be seen clearly that the striations are parallel to a ⟨110⟩ direction.

On the basis of a large number of observations on 2024 and 7075 it can be said that in the aluminum alloys the striations are parallel to a ⟨110⟩ direction within $\pm 10°$ and the plane of fracture is also close to a (100) plane. The same observations also show that the lower the growth rates, the more crystallographic the fatigue fracture.

In high stacking fault materials (aluminum alloys) the fatigue crack front within a grain is slightly curved, lagging behind along the grain boundaries. This curvature however is very slight in the case of the high strength aluminum alloys, at least for growth rates below 10^{-4} inches/cycle. Forsyth [1] suggested the faster rate of propagation in the center of the grains was due to the ease of cross slip away from the grain boundaries. It is felt that this argument is not valid. It seems rather that the proximity of a neighboring grain will allow more slip systems to operate and a given crack tip opening displacement will be accommodated by a smaller crack extension if shear can take place on the four slip planes available (see Fig. 2 and add 2 slip planes in and out of the plane of the drawing). In our observations the slight curvature of the crack front along the grain boundary does not seem to influence the overall crystallographic orientation of the crack front across the grain.

Fatigue crack propagation in vacuum and in air

Meyn [3] was the first to observe that striations were not formed during fatigue crack propagation in vacuum. In order to duplicate Meyn's results tests were run successively in air, vacuum of 5×10^{-6} and air with 2024 T3, 7075 T6 and Ti-6Al-4V and in each case striations were completely

absent on the fracture surface created during crack propagation in vacuum. The crack growth rates in vacuum were such that if striations had been present they could have been easily resolved.

Fig. 7 shows clearly the absence of striations when testing is done in vacuum; the etch pits show that there is no marked difference between the orientation of the plane of fracture in air and vacuum. The transition from striations (air) to no striations (vacuum) is abruptly marked. This was verified by a test in which 5 cycles were applied sucessively in air, vacuum, air etc. Five well defined fatigue striations were present in between the two featureless fracture surfaces produced in vacuum. All the observations, limited to growth rates below 5 microns/cycle, confirmed the absence of fatigue striations in vacuum. It was concluded that fatigue striations were the result of an environment factor and not created by plastic blunting as suggested by Laird [2]. However, Laird's mechanism may be operative at large growth rates (>10 microns cycle).

The mechanism of crack extension by alternating shear shown on Fig. 2 is reversible unless an oxide film is formed and blocks reversed slip. Fig. 8 shows the model proposed to explain the formation of the fatigue striation as a consequence of the oxidation at the crack tip. The finite growth rate observed in vacuum is due to the physical irreversibility of plastic deformation. Plasticity theory requires a completely reversible deformation and would predict no fatigue crack growth in vacuum.

The model presented on Fig. 8 also accounts for the profiles of the fatigue striation consistently observed in aluminum alloys [12]. Stereo micrographs and a study of the shadowing contrast of replicas of matching faces of the fracture surfaces show that the striations are in anti-register, i.e. peaks match peaks and valleys match valleys. Naturally the ridges are not always as sharply defined as on the sketch.

The irreversible slip model of formation of fatigue striation shows that some ambiguity may exist in determining the influence of an environment on the rate of fatigue crack propagation. The total extension per cycle may be changed, or only the amount of reversible slip may be affected by the environment. For instance Bradshaw and Wheeler [13] report a large change in growth rates for an Al-Cu-Mg alloy (2024T3) between dry air and laboratory air tests. The difference is attributed to the corrosive influence of water vapor. However ductile striations are formed in both environments and also in distilled water and sea water with that alloy. It could also be concluded that the environment, by modifying the thickness and strength of the oxide film at the crack tip, limits the amount of reversible slip to a smaller value than in dry air.

Corrosion fatigue and brittle striations

Since brittle striations were reported by Forsyth [1] to form mainly with Al-Zn-Mg alloys in a corrosive environment a 7075 alloy was tested in am-

biant air, distilled water and 3% KCl solution. The tests were tension-tension at 72 °/min, using single edge notched specimens the fatigue crack being always started in air in order to follow the change of the striation morphology with the environment. The 7075 alloy was tested in the following heat treated conditions:

water quenched	WQ	R_b 49
under aged	UA(2 hr at 250 °F)	R_b 86
peak aged	PA(24 hr at 250 °F)	R_b 94
over aged 1	OA1(PA + 9 hr at 350 °F)	R_b 86
over aged 2	OA2(PA + 54 hr at 350 °F)	R_b 75

The slip distribution is markedly affected by heat treatment. In the water quenched and overaged conditions slip is uniformly distributed throughout the grains. In the underaged and peak aged conditions the precipitates are coherent and slip is concentrated in narrow, straight slip bands because the flow stress in the slip band is lowered once the precipitates have been sheared. In the overaged alloys the incoherent precipitates are by-passed by finely dispersed slip [17].

The difference in propagation rates as a function of aging in the three environments is shown in Fig. 9 for $\Delta K = 15$ ksi $\sqrt{\text{in}}$. In all cases the fracture path is transgranular. Aging does not markedly affect the growth rate in air and ductile striations are always present throughout the fracture surfaces. In distilled water ductile striations are observed in the water quenched and overaged alloys and brittle striations in the under and peak aged alloys. In the salt solutions fracture is always accompanied by the formation of brittle striations except for the water quenched alloy which exhibit ductile striations.

The brittle striations shown in B on Fig. 1 are typical of all the brittle striations formed in the different environments. The fracture appears to be a cleavage fracture along a (100) plane or a plane very close to it. Short river markings indicate the direction of crack propagation. The line marking the arrest of the crack front at each cycle is not always well defined indicating that the shear component of fracture is very small.

The effect of anodic and cathodic polarization was studied by impressing a 500 microamp current to the test specimen. Since the outer surfaces of the specimen were coated with epoxy, this corresponded to an average current density of 1 milliamp/cm^2 on the fracture surface. The polarity of the current was reversed every 12 cycles (10 seconds) without interrupting the cycling test. Fig. 10 reproduces a typical recording of current and corrosion potential (versus a saturated calomel electrode). A similar technique was used by Forsyth [14] to study intergranular corrosion fatigue. The marked change in growth rates with corrosion potential can be seen from the change in striation spacings in Fig. 11 which represents the fracture

surface of an overaged 7075 alloy. The change in striation spacing is associated with a change from ductile (shear) striations to brittle (cleavage) striations. This change is abrupt and corresponds to a corrosion potential of –1·3 volt which can be determined from Fig. 10 after a count of ductile and brittle striations present in each band has been made. The change in the mode of fracture from shear to cleavage is often accompanied by a change in the orientation of the fracture plane within a single grain. Fig. 12 shows this kind of behavior for a 2024 T3 alloy, the difference in shadowing contrast of each plateau indicating the change of orientation of the fracture plane. When the specimen is anodic, fracture by cleavage will follow the nearest available (100) plane even if it is not quite normal to the tensile axis. As soon as cathodic protection stops the cleavage fracture, ductile striations are formed by shear and the fracture plane returns to an orientation normal to the tensile axis.

Discussion

The marked changes in fatigue growth rates in a salt solution with changes of corrosion potential lead to the conclusion that corrosion fatigue cracking is in part an electrochemical process. However, it is not a process of dissolution or of embrittlement of the material ahead of the crack tip because of the sharp change in the striation spacing between anodic and cathodic fracture zones. Corrosion fatigue can best be explained by a mechanism of stress sorption cracking i.e. weakening of the metal bonds at the crack tip through adsorption of the environment or its constituents. If the adsorption process leads to a reduction of the cohesive strength σ, the change from ductile to brittle fracture behavior with current reversals can be accounted for on the basis of arguments presented by Kelly [15] and Westwood [16]. Kelly suggests that if the ratio of the larger tensile stress to the largest shear stress close to the crack tip is greater than the ratio of the ideal cleavage stress to the ideal shear stress then fracture takes place by cleavage. If the reverse is true some plastic flow will take place at the crack tip. When the corrosion potential is changed from cathodic to anodic the stress distribution at the crack tip does not change but adsorption of the environment constituents may lower the tensile cohesive strength of the atomic bonds resulting in fracture by cleavage. By the same argument the influence of aging on corrosion fatigue susceptibility may be explained by the dependence of the maximum shear stress at the crack tip on the shear strength and slip character of the alloy. In the underaged and peak alloys, concentrated slip in narrow slip bands in which coherent precipitates have been sheared will result in a lower maximum shear stress at the crack tip than in the case of the overaged alloys. Hence the susceptibility of the underaged and peak aged alloys to cleave in the presence of an environment.

The difference in growth rates and fracture features between the vacuum and air environment certainly stresses the role played by the oxide film at the crack tip. In the case of a liquid environment a pseudo-Rebinder effect could be operative at the crack tip, the mobility of the dislocations escaping to create crack extension being strongly dependent upon adsorbed species. The mechanisms by which the pinning of surface dislocations by adsorbates could contribute to fracture by cleavage at the tip of a crack remain to be postulated.

Acknowledgments

The author would like to acknowledge the suggestions of H. Brunner, the fruitful discussions with T. R. Beck, F. A. McClintock, M. O. Speidel and the technical help of R. Lee, P. Olson and H. Wallner.

References

1. FORSYTH, P. J. E., *Acta Metallurgica*, vol. 11, July 1963, p. 703.
2. LAIRD, C., ASTM STP 415, 1967, p. 131.
3. HERTZBERG, R. W., ASTM STP 415, 1967, p. 205.
4. MEYN, D. A., *Trans. ASM*, vol. 61, No. 1, March 1968, p. 42.
5. McCLINTOCK, F. A., PELLOUX, R., Boeing Scientific Research Laboratories Document D1-82-0708, February 1968.
6. BEACHEM, C. D., MEYER, D. A., ASTM Preprint No. 41, ASTM Meeting, Boston, Mass., June 1967.
7. McCLINTOCK, F. A., ASTM STP 415, 1967, p. 169.
8. WILLIAMS, M. L., *Trans ASME Journal of Applied Mechanics*, 1957.
9. RICE, J. R., ASTM STP 415, 1967, p. 247.
10. WILHEM, D. P., ASTM STP 415, 1967, p. 363.
11. SPITZIG, W. A., WEI, R. P., *Trans ASM*, vol. 60, No. 3, Sept. 1967, p. 279.
12. McMILLAN, J. C., PELLOUX, R. M. N., ASTM STP 415, 1967, p. 505.
13. BRADSHAW, F. J., WHEELER, C., *Applied Materials Research*, April 1966. p. 112.
14. FORSYTH, P. J. E., SAMPSON, E. G. F., RAE Tech. Report 65158, August 1965.
15. KELLY, A., TYSON, W. R., COTTRELL, A. H., *Phil Mag.* vol. 15, 1967, p. 567.
16. KAMDAR, M. H., WESTWOOD, A. R. C., *Phil. Mag.* vol. 15, 1967, p. 641.
17. SPEIDEL, M. O., 'Interaction of dislocations with precipitates in high strength aluminum alloys and susceptibility to stress corrosion cracking', paper presented at the Conference on Fundamental Aspects of Stress Corrosion Cracking, Ohio State University, Columbus, Ohio, Sept. 11-15, 1967.

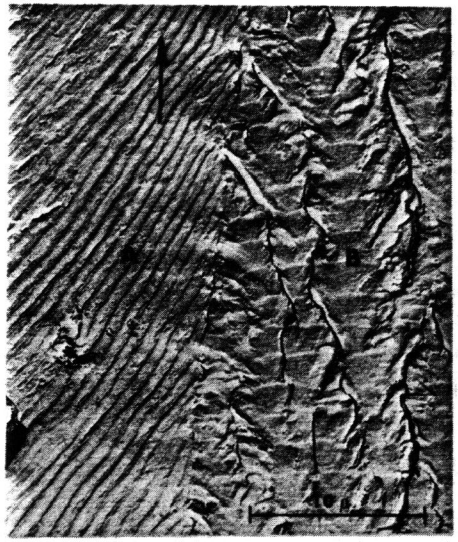

Fig. 1. Fracture surface of an Al-Zn-Mg alloy tested in fatigue in distilled water at room temperature. Ductile striations in grain A. Brittle striations in grain B. The direction of crack propagation is indicated by an arrow.

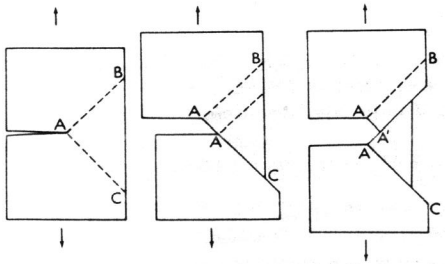

Fig. 2. Crack extension by alternating shear in a singly grooved tensile specimen.

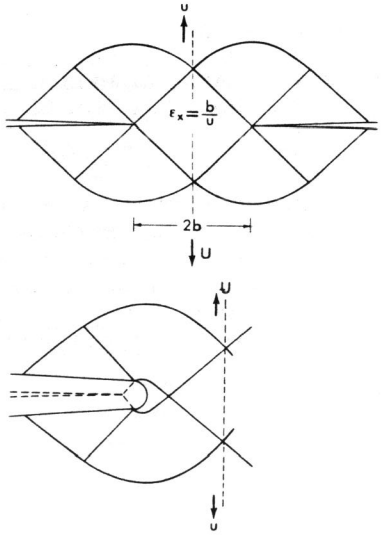

Fig. 3. Slipline flow field for a notched, doubly grooved tensile specimen.
a. prior to blunting
b. after blunting.

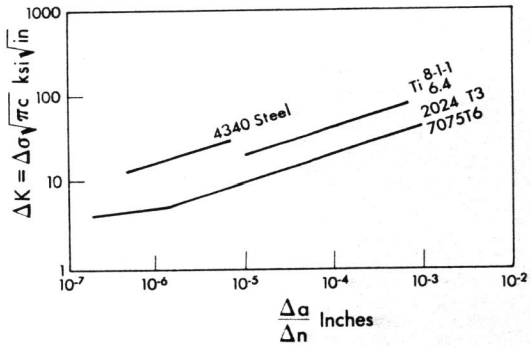

Fig. 4. Fatigue crack growth data versus change of stress intensity factor for aluminum alloys, titanium alloys and 4340 steels.

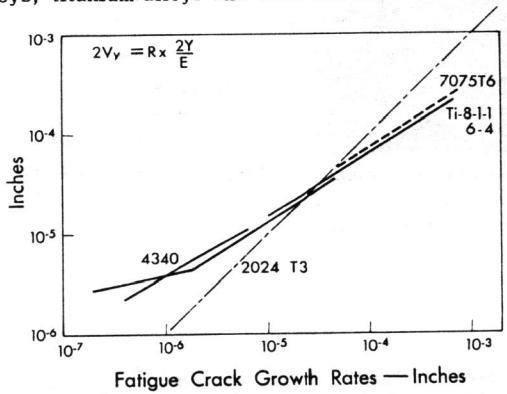

Fig. 5. Crack tip opening displacement versus fatigue crack growth rates for aluminum and titanium alloys and 4340 steels.

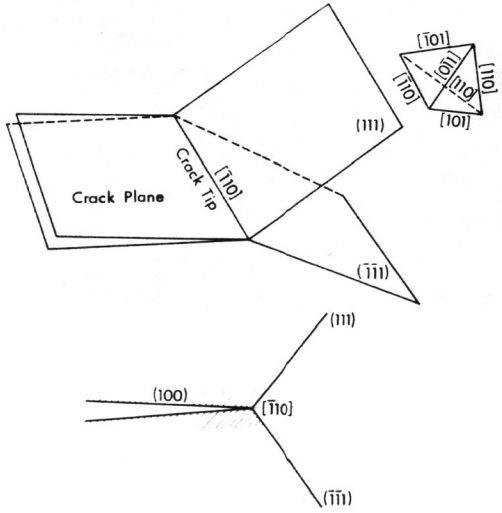

Fig. 6. Crystallographic orientation of fracture plane, crack tip direction and slip planes.

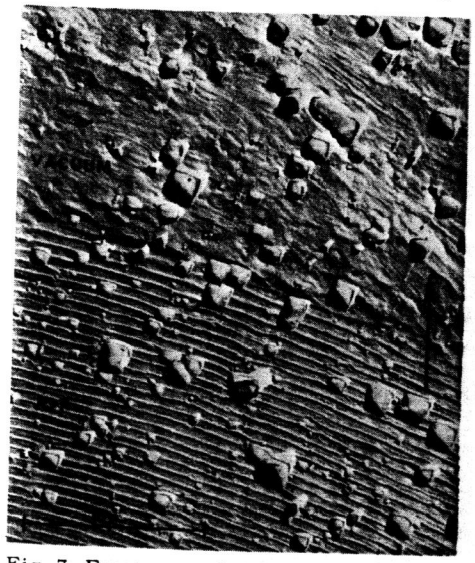

Fig. 7. Fracture surface of 2024T3 aluminum alloy tested in fatigue first in air, then in vacuum of 5×10^{-6} Torr-fatigue striations are not formed in vacuum. The etch pits indicate a (100) plane of fracture and a 110 striation orientation.

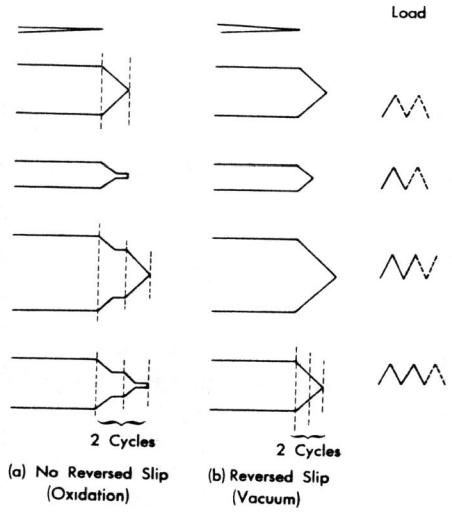

Fig. 8. Model comparing crack tip extension after 2 load cycles in air and in vacuum.

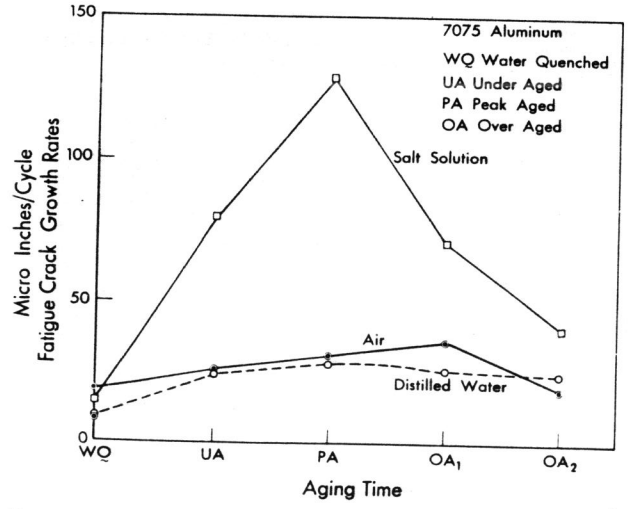

Fig. 9. Fatigue crack growth rates at $\Delta K = 15$ ksi $\sqrt{\text{in.}}$ in air, distilled water and sea water as a function of aging treatment for 7075 alloy.

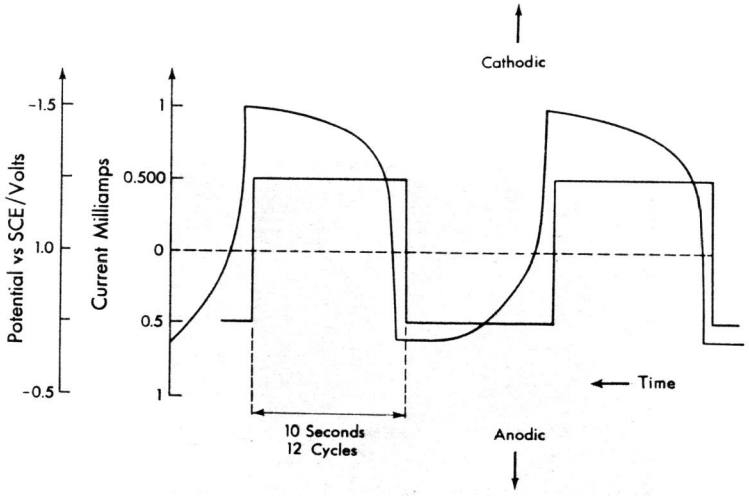

Fig. 10. Recording of corrosion current and potential of a fatigue test under controlled corrosion conditions (the displacement of current and potential recording along the x axis is due to the use of a two pen recorder).

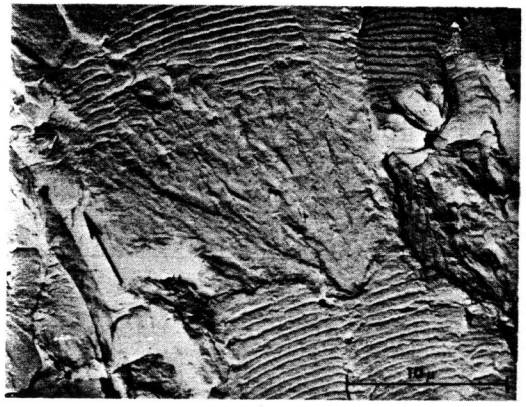

Fig. 11. Fracture surface of 7075 overaged alloy tested in sea water. Transition from ductile to brittle striations and back to ductile striations when the corrosion current is changed from cathodic to anodic and back to cathodic.

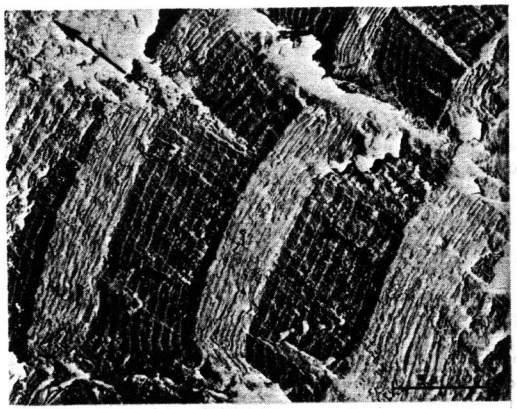

Fig. 12. Fracture surface of 2024 aluminum alloy tested in sea water. The orientation of the fracture plane is changing at each current reversal making the specimen anodic, cathodic, anodic.